Adsorption properties of a colloid-polymer mixture confined in a slit pore

Soon-Chul Kim*
Department of Physics, Andong National University, Andong, 760-749 Korea

Peter T. Cummings
Department of Chemical Engineering, University of Tennessee, Knoxville, Tennessee, 37996
and Chemical Technology Division, Oak Ridge National Laboratory, Oak Ridge, Tennessee 37831
(Received 5 January 2001; published 24 September 2001)

The soft fundamental-measure theory, which was based on the additive colloid-polymer mixture [M. Schmidt, Phys. Rev. E **62**, 3799 (2000)] has been employed to investigate the adsorption of a colloid-polymer mixture within a hard slit pore. The calculated results show that the adsorption for the confined colloid-polymer mixture is very different from those of the colloid-colloid and polymer-polymer mixtures. The equilibrium particle density distribution strongly depends on the softness of a star polymer. The local relative concentration oscillates with a spatial period close to the diameter of a large particle in the same way as the equilibrium particle density distribution. The size selectivity in adsorption depends both on the softness of a star polymer and on the particle size ratio in a binary mixture. In particular, the strong adsorption occurs at the ultra-soft polymer and high bulk packing fraction.

DOI: 10.1103/PhysRevE.64.041507 PACS number(s): 61.20.−p, 05.20.Jj, 64.75.+g

I. INTRODUCTION

Over the last decade, the density functional theory of classical fluids has evolved into an efficient theoretical tool for studying confined fluid mixtures [1–4]. Many different kinds of theories have been developed for dealing with problems such as phase separation and interfacial adsorption of mixtures in the confined systems [5]. For the hard-sphere mixture, the newest and most successful approximation is the fundamental-measure theory which was developed by Rosenfeld and co-workers [6,7]. The density functional approximations for various common model fluids, within the soft fundamental-measure theory, was proposed to study the structural properties in the fluid phase [8,10,9]. More recently, Schmidt [11] proposed a soft fundamental-measure theory for a model colloid-polymer mixture of particles interacting with a radially symmetric pair potential. In this case, the cross interaction between unlike species can be described by the fundamental-measure theory for the hard-sphere and star polymer. These interactions turn out to have a physically reasonable form [12,13]. Schmidt applied it to investigate the partial pair distribution function $g_{ij}(r,\rho)$ of an additive colloid-polymer mixture, and obtained reasonably good results compared with the computer simulation. Furthermore, a fundamental-measure theory for a nonadditive model colloid-polymer mixture was developed by Schmidt *et al.* [14]. Rosenfeld *et al.* [15] compared the soft fundamental measure theory and the computer simulation for the pair correlation function in the fluid phase of penetrable spheres by using the test-particle limit. They showed that the penetrable sphere functional is quite successful.

Kim [16] recently extended the soft fundamental-measure theory of Schmidt [11] for the polydisperse soft-sphere fluid, and applied it to study the adsorption properties of a confined polydisperse soft-sphere fluid. He showed that the preferred species in a slit pore depends on the pore size and softness of a polydisperse soft-sphere fluid. The local relative concentration oscillates with a spatial period close to the diameter of a large particle in the same way as the equilibrium particle density distribution. The results suggest that the pore average mole fraction and local relative concentration for colloidal hard spheres mixed with star polymers are affected by the softness of a star polymer. It is generally expected that the colloid-polymer mixture shows very different adsorption properties compared with binary mixtures such as colloid-colloid and polymer-polymer mixtures, because of the softness of a star polymer. On the other hand, the adsorption behavior of an open system is very different from that of the closed system such as the spherical pore, where the number of particles N is fixed [17].

This paper is arranged as follows. In Sec. II, we will briefly summarize the soft fundamental-measure theory for the additive colloid-polymer mixture, and derive the density profile equation for the colloid-polymer mixture confined in a structureless hard slit pore. In Sec. III, the local relative concentration, i.e., the local size segregation and pore average mole fraction, which represents the size selectivity in adsorption of the confined colloid-polymer mixtures, is studied theoretically and compared with the confined colloid-colloid and polymer-polymer mixtures in detail. Finally, the pore size and particle size dependence for confined colloid-polymer mixtures are also discussed.

II. THEORY

In the density functional theory for colloidal hard spheres mixed with star polymers with the particle diameter σ_i [here σ_c and σ_p denote the diameters of the colloidal hard sphere and the polymer, respectively], the equilibrium particle density distribution $\rho_i(\vec{r})$ of the inhomogeneous fluid is described by the minimum of the grand canonical potential

*Email address: sckim@andong.ac.kr

$\Omega[\rho]$ satisfying the Euler-Lagrange relation $\delta\beta\Omega[\rho_c,\rho_p]/\delta\rho_i(\vec{r})=0$, where $\beta=1/k_BT$ is the inverse temperature and k_B is Boltzmann's constant [19]. If the inhomogeneous fluid is in contact with the homogeneous bulk fluid, its chemical potential μ_i is equal to that of the homogeneous bulk fluid. After some manipulations, the equilibrium particle density distribution function (or density profile equation) $\rho_i(\vec{r})$ is given by

$$\rho_i(\vec{r})=\rho_i \exp[-\beta u_i^{\mathrm{ext}}(\vec{r})+c_i^{(1)}(\vec{r};[\rho_c,\rho_p]) - c_i^{(1)}(\rho_c,\rho_p)] \quad \text{for } i=c,p, \tag{1}$$

where ρ_i denotes the homogeneous bulk density, and $u_i^{\mathrm{ext}}(\vec{r})$ is an external potential acting on species σ_i [19,20]. In Eq. (1), $c_i^{(1)}(\vec{r};[\rho_c,\rho_p])$ is the one-particle direct correlation function (DCF) of the inhomogeneous colloid-polymer mixture, which is defined as

$$c_i^{(1)}(\vec{r};[\rho_c,\rho_p])=-\frac{\delta\beta F_{\mathrm{ex}}[\rho_c,\rho_p]}{\delta\rho_i(\vec{r})}, \tag{2}$$

where $F_{\mathrm{ex}}[\rho_c,\rho_p]$ is the excess free energy functional of the system, and $c_i^{(1)}(\rho_c,\rho_p)$ is the one-particle DCF of the homogeneous colloid-polymer mixture.

Following Schmidt's expression [11], we assume an excess free energy functional $F_{\mathrm{ex}}[\rho_c,\rho_p]$ such that

$$F_{\mathrm{ex}}[\rho_c,\rho_p]=k_BT\int d\vec{s}\,\Phi[n_\alpha(\vec{s})]. \tag{3}$$

where $\Phi[n_\alpha(\vec{s})]$ is the excess free energy per volume. Then the one-particle DCF $c_i^{(1)}(\vec{r};[\rho_c,\rho_p])$ is simply given, from Eqs. (2) and (3), as

$$c_i^{(1)}(\vec{r};[\rho_c,\rho_p])=-\int d\vec{s}\sum_\alpha \frac{\partial\Phi[n_\gamma(\vec{s})]}{\partial n_\alpha(\vec{r})}\omega_i^{(\alpha)}(|\vec{r}-\vec{s}|), \tag{4}$$

where the system-averaged fundamental geometric measure of the particles $n_\alpha(\vec{r})$ is given by

$$n_\alpha(\vec{r})=\sum_{i=1}^{2}\int d\vec{s}\,\rho_i(\vec{s})\omega_i^{(\alpha)}(|\vec{r}-\vec{s}|). \tag{5}$$

$\omega_i^{(\alpha)}(r)$ are weight functions, and the excess free energy $\Phi[n_\alpha(\vec{r})]$ per volume is assumed as

$$\Phi[n_\alpha(\vec{r})]=-n_0(\vec{r})\ln[1-n_3(\vec{r})] + \frac{n_1(\vec{r})n_2(\vec{r})-\vec{n}_{v1}(\vec{r})\cdot\vec{n}_{v2}(\vec{r})}{1-n_3(\vec{r})} + \frac{n_2(\vec{r})^3[1-(\vec{n}_{v2}(\vec{r})/n_2(\vec{r}))^2]^3}{24\pi[1-n_3(\vec{r})]^2}. \tag{6}$$

Actually, the excess free energy function with the tensorial weight densities [7] can be introduced, which leads to superior results in highly inhomogeneous situations such as the crystalline phase. However, we have chosen the soft fundamental-measure theory introduced by Schmidt to investigate the structural properties of a colloid-polymer mixture, because it yields very reasonable results for the structural properties of a soft-sphere fluid. The set of weight functions appeared in Eqs. (4) and (5) is related to the generating function $\omega_i^{(3)}(r)$ through

$$\omega_i^{(2)}(r)=-\frac{\partial\omega_i^{(3)}(r)}{\partial r}, \quad \vec{\omega}_i^{(v2)}(\vec{r})=\omega_i^{(2)}(r)\frac{\vec{r}}{r},$$

$$\omega_i^{(1)}(r)=\frac{\omega_i^{(2)}(r)}{4\pi r}, \quad \vec{\omega}_i^{(v1)}(\vec{r})=\omega_i^{(1)}(r)\frac{\vec{r}}{r}, \tag{7}$$

$$\omega_i^{(0)}(r)=\frac{\omega_i^{(1)}(r)}{r},$$

where $\omega_i^{(3)}$, $\omega_i^{(2)}$, $\omega_i^{(1)}$, and $\omega_i^{(0)}$ are scalar quantities and $\vec{\omega}_i^{(v2)}$ and $\vec{\omega}_i^{(v1)}$ are vectors. The generating weight function $\omega_i^{(3)}(r)$ is determined by solving the deconvolution equation, which is an integrodifferential equation [11].

For the specific form of a intermolecular potential such as a colloidal hard sphere mixed with a star polymer, a simple generating weight function can be obtained [11]. Following the colloid-polymer model proposed by Schmidt, we choose the pairwise potentials between colloidal hard-sphere and star polymer as follows: (i) The interaction between the star polymer $\beta u_{pp}(r)$ consists of a logarithmic potential for small distances,

$$\beta u_{pp}(r)=\begin{cases} -2q\ln(r/R_p)+\ln\binom{2q}{q}, & 0<r<R_p \\ \phi_q(r)+\ln\binom{2q}{q}, & R_p<r<2R_p \\ 0, & 2R_p<r, \end{cases} \tag{8}$$

where $\binom{2q}{q}$ is the binomial coefficient, and q denotes the softness of a star polymer. The crossover function between small and large distances $\phi_q(r)$ is given by

$$\phi_q(r)=-\ln[(1+\xi)^{2q}-\xi^{q+1}B_q\,{}_2F_1(1,1-q;2+q;-\xi)],$$

where $\xi=(r/R_p)-1$, $B_q=2\Gamma(1+2q)\Gamma^{-1}(q)\Gamma^{-1}(2+q)$, and ${}_2F_1$ is the hypergeometric function. (ii) The hard sphere interaction $\beta u_{cc}(r)$ has been assumed for the colloid-colloid interaction:

$$\beta u_{cc}(r)=\infty, \quad 0<r<R_c,$$

$$=0, \quad 2R_c<r. \tag{9}$$

(iii) The colloid-polymer interaction $\beta u_{cp}(r)$ is assumed to have a hard core due to excluded volume induced by a colloid and an additional logarithmic repulsion:

$$\beta u_{cp}(r)=\infty, \quad r<R_c,$$

$$=-q\ln\left(\frac{r-R_c}{R_s}\right), \quad R_c<r<R_c+R_p,$$

$$=0, \quad \text{otherwise.} \tag{10}$$

Here note that the colloidal and polymer are simplified with the central forces.

For the above intermolecular potentials [Eqs. (8)–(10)], the generating weight function $\omega_c^{(3)}(r)$ for the colloidal hard-sphere case [8] is identical to the pure hard-sphere case

$$\omega_c^{(3)}(r)=\theta(R_c-r), \tag{11}$$

where $\theta(r)$ is the Heaviside step function. The generating weight function $\omega_p^{(3)}(r)$ for the polymer is given by

$$\omega_p^{(3)}(r)=1-(r/R_p)^q, \quad 0<r<R_p,$$

$$=0, \quad \text{otherwise,} \tag{12}$$

where q represents the softness of a polymer. In the limit $q\rightarrow\infty$ the weight function [Eq. (12)] approaches a step function $\omega_p^{(3)}(r)=\theta(R_p-r)$, and the potential becomes a hard core with the radius R_p. Equations (7), (11), and (12) constitute the set of weight functions for colloidal hard spheres and star polymers.

For the homogeneous star polymer, the one-particle DCF $c_p^{(1)}(\rho_c,\rho_p)$ becomes, from Eqs. (4), (6), and (7),

$$c_p^{(1)}(\rho_c,\rho_p)=\ln(1-n_3)-\frac{4\pi R_p^3 n_0}{1-n_3}\left[\frac{1}{3}-\frac{1}{q+3}\right]-\frac{qR_p}{1-n_3}\left[\frac{n_2}{q+1}+\frac{4\pi R_p n_1}{q+2}\right]-\frac{4\pi R_p^3 n_1 n_2}{(1-n_3)^2}\times\left[\frac{1}{3}-\frac{1}{q+3}\right]-\frac{R_p^2 n_2^2}{2(1-n_3)^2}\left[\frac{q}{q+2}\right]-\frac{R_p^3 n_2^3}{3(1-n_3)^3}\left[\frac{1}{3}-\frac{1}{q+3}\right], \tag{13}$$

with

$$n_0=\rho_c+\rho_p, \quad n_1=\rho_c R_c+\frac{q}{q+1}\rho_p R_p,$$

$$n_2=4\pi\rho_c R_c^2+\frac{4\pi q}{q+2}\rho_p R_p^2 \tag{14}$$

and

$$n_3=\frac{4\pi}{3}\rho_c R_c^3+4\pi\left[\frac{1}{3}-\frac{1}{q+3}\right]\rho_p R_p^3,$$

since $\rho_p(\vec{r})=\rho_p$ and $\rho_c(\vec{r})=\rho_c$ for the homogeneous colloid-polymer mixture. Note here that the one-particle DCF $c_p^{(1)}(\rho_c,\rho_p)$ for the star polymer is a function of the bulk densities of a star polymer as well as a colloidal hard sphere. The one-particle DCF $c_c^{(1)}(\rho_c,\rho_s)$, corresponding to a colloidal hard sphere, becomes

$$c_c^{(1)}(\rho_c,\rho_s)=\ln(1-n_3)-\frac{\pi R_c^3 n_0}{3(1-n_3)}-\frac{R_c}{1-n_3}\left[\frac{n_2}{2}+\frac{\pi R_c n_1}{4}\right]-\frac{4\pi R_c^3 n_1 n_2}{3(1-n_3)^2}-\frac{R_c^2 n_2^2}{2(1-n_3)^2}-\frac{R_c^3 n_2^3}{9(1-n_3)^3}. \tag{15}$$

The combined equations (1), (4), (13), and (15) constitute the density profile equation for an additive colloid-polymer mixture.

On the other hand, for an (additive) colloid-colloid mixture the one-particle DCF $c_i^{(1)}(\rho_1,\rho_2)$ [6] becomes

$$c_i^{(1)}(\rho_1,\rho_2)=\ln(1-n_3)-\frac{4\pi R_i^3 n_0}{3(1-n_3)}-\frac{R_i n_2}{1-n_3}-\frac{4\pi R_i^2 n_1}{1-n_3}-\frac{4\pi R_i^3 n_1 n_2}{3(1-n_3)^2}-\frac{R_i^2 n_2^2}{2(1-n_3)^2}-\frac{R_i^3 n_2^3}{9(1-n_3)^3} \quad \text{for} \quad i=1,2, \tag{16}$$

with

$$n_0=\sum_{i=1}^{2}\rho_i, \quad n_1=\sum_{i=1}^{2}\rho_i R_i, \quad n_2=\sum_{i=1}^{2}4\pi\rho_i R_i^2,$$

$$n_3=\sum_{i=1}^{2}\frac{4\pi}{3}\rho_i R_i^3.$$

Many authors [6,17,18] showed that, for a confined colloid-colloid mixture, the fundamental-measure theory yields very good results compared with the computer simulation.

For the (additive) polymer-polymer mixture, the one-particle DCF $c_i^{(1)}(\rho_1,\rho_2)$ becomes

$$c_i^{(1)}(\rho_1,\rho_2)=\ln(1-n_3)-4\pi\left[\frac{1}{3}-\frac{1}{q+3}\right]\frac{R_i^3 n_0}{(1-n_3)}-\frac{qR_i n_2}{(q+1)(1-n_3)}-\frac{4\pi q R_i n_1}{(q+2)(1-n_3)}-4\pi\left[\frac{1}{3}-\frac{1}{q+3}\right]\frac{R_i^3 n_1 n_2}{(1-n_3)^2}-\frac{qR_i^2 n_2^2}{2(q+2)(1-n_3)^2}-\left[\frac{1}{3}-\frac{1}{q+3}\right]\frac{R_i^3 n_2^3}{3(1-n_3)^3} \quad \text{for } i=1 \text{ and } 2, \tag{17}$$

with

$$n_0=\sum_{i=1}^{2}\rho_i, \quad n_1=\sum_{i=1}^{2}\frac{q}{q+1}\rho_i R_i,$$

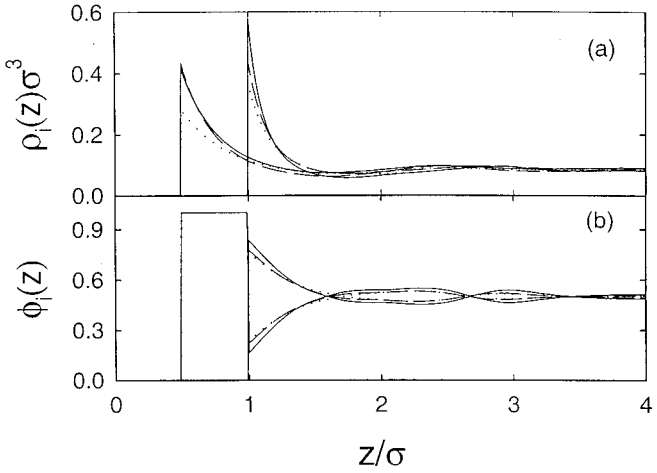

FIG. 1. (a) Equilibrium particle density distribution $\rho_i(z)\sigma^3$ for the binary fluid mixtures confined in a slit pore with $L=8.0\sigma$, $\eta=0.394$, and $x=0.5$; dotted lines represent a polymer-polymer mixture ($q=12$ and $\sigma_p/\sigma_p=0.5$), dashed lines a colloid-polymer mixture ($q=12$ and $\sigma_c/\sigma_p=0.5$), and solid lines a colloid-colloid (mixture $\sigma_c/\sigma_c=0.5$). (b) Local relative concentration $\phi_i(z)$.

$$n_2=\sum_{i=1}^{2}\frac{4\pi q}{q+2}\rho_i R_i^2, \quad n_3=\sum_{i=1}^{2}4\pi\left[\frac{1}{3}-\frac{1}{q+3}\right]\rho_i R_i^3.$$

Note here that the polymer-polymer mixture was recently extended to investigate the adsorption properties of confined polydisperse soft-sphere fluid with the continuous particle distribution [16].

For the structureless hard slit pore, the external potential $\beta u_i^{\text{ext}}(z)$ is simply given as

$$\beta u_i^{\text{ext}}(z)=0, \quad R_i<z<L-R_i,$$
$$=\infty, \quad \text{otherwise}, \tag{18}$$

where L and z are the width of the slit pore and distance from a hard slit wall, respectively. The maximum distances available to the center of a colloidal hard sphere or a star polymer are $L-R_i$. Then all quantities only depend on the z axis, but not on x and y; $\rho_i(\vec{r})=\rho_i(z)$, and so on. The equilibrium particle density distribution function [Eq. (1)] becomes

$$\rho_i(z)=\rho_i\exp[-\beta u_1^{\text{ext}}(z)+c_i^{(1)}(z;[\rho_c,\rho_p])-c_i^{(1)}(\rho_c,\rho_p)], \tag{19}$$

with

$$c_i^{(1)}(z;[\rho_c,\rho_p])=2\pi\int_0^\infty dR\,Rc_i^{(1)}(\sqrt{R^2+z^2};[\rho_c,\rho_p]). \tag{20}$$

III. RESULTS AND DISCUSSION

The equilibrium particle density distribution $\rho_i(z)\sigma_i^3$ and its corresponding local relative concentration $\phi_i(z)$ for the binary fluid mixtures are displayed in Fig. 1 as a function of the distance from a hard slit wall, where the packing fraction η for the binary fluid mixture is given as $\eta=\pi\Sigma_{i=1}^{2}\rho_i\sigma_i^3/6$. The particle diameter σ has been taken to be the unit of a length, and the bulk mole fraction $x=\rho_1/\Sigma_{i=1}^{2}\rho_i$ is 1/2. Actually, the size of a colloidal sphere is not large compared to that of a polymer. However, here we used a relatively small sphere for the colloidal particle to study the size effect in adsorption properties of a colloid-polymer mixture [21]. As can be seen from Fig. 1(a), the calculated equilibrium particle density distribution strongly depends on the intermolecular interaction between two particles. For the large-q value, i.e., the strong repulsive interaction between the star polymers, a higher particle density distribution developed near a slit pore; for the colloid-colloid mixture a higher particle density distribution can be found near a hard slit pore, this is to be compared with the polymer-polymer mixture, which has a soft-sphere interaction between two particles. An interesting fact is that, in a colloid-polymer mixture, the particle density distribution for the polymer is lower compared with that for a colloidal hard sphere in a colloid-colloid mixture because of the softness of a polymer; however, the particle density distribution for a colloidal hard sphere is almost the same as that in the colloid-colloid mixture. These results suggest that in a colloid-polymer mixture the equilibrium particle density distribution depends strongly on the softness of a star polymer. As for the equilibrium particle density distribution, the distance between the two peaks is also almost the same as the diameter of a star polymer. In Fig. 1(b), the local relative concentration or concentration profile $\phi_i(z)$ is displayed, which is defined as

$$\phi_i(z)=\frac{\rho_i(z)}{\sum_{i=1}^{2}\rho_i(z)}, \tag{21}$$

where the local relative concentration represents the effect of the local size segregation between particles of different species [22]. It is expected that the strong local relative concentration is related to the large particle density difference between two particles. As can be seen from Fig. 1(b), the calculated local relative concentration shows the strong local size segregation with local cross correlation between particles of different sizes around the bulk mole fraction ($x=1/2$) in the relative amounts of small and large particles. Strong local size segregation near a slit pore was developed for a colloid-colloid mixture with a strong repulsive interaction compared with that of a polymer-polymer mixture. This means that the large size selectivity in adsorption depends on the softness of a star polymer. The local relative concentration oscillates with a spatial peak close to the diameter of a star polymer with a large diameter, in the same way as the equilibrium particle density distribution does. In particular, Roth and Dietrich recently showed that for a colloid-colloid mixture near a hard wall the oscillatory behavior obtained by the fundamental-measure theory agrees excellently with the computer simulation [18].

In Fig. 2 we show the calculated equilibrium particle density distribution and its corresponding local relative concentration for binary fluid mixtures with different particle size

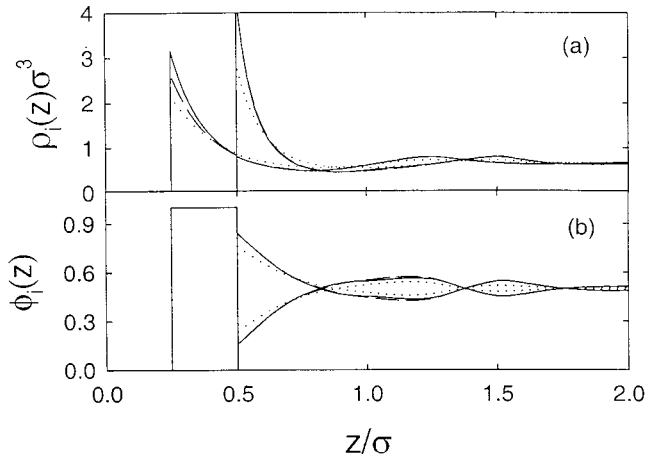

FIG. 2. Same as in Fig. 1; dotted lines represent a polymer-polymer mixture ($q=12$ and $\sigma_p/\sigma_p=2.0$), dashed lines a colloid-polymer mixture ($q=12$ and $\sigma_c/\sigma_p=2.0$), and solid lines a colloid-colloid mixture ($\sigma_c/\sigma_c=2.0$).

ratios. As can be seen from Fig. 2, the equilibrium particle density distribution depends on the intermolecular potential between two particles. Higher particle density distributions are developed for the colloidal hard sphere, while lower particle density distributions are found in a star polymer. In particular, the particle density distribution for a colloidal hard sphere in a colloid-colloid mixture is almost the same as that of a colloidal hard sphere in a colloid-polymer mixture. For the small particle size ratio the effect of softness is smaller than that in the large particle size ratio. However, a comparison with Fig. 1 shows that the local size segregation depends both on the particle size ratio and on the softness of a star polymer. The local relative concentration oscillates with a spatial peak close to the diameter of a large particle, as does the equilibrium particle density distribution.

The pore average mole fraction ϕ_i for the binary fluid mixture is displayed in Fig. 3 as a function of the slit width L/σ. Here the pore average mole fraction ϕ_i is defined as

$$\phi_i=\frac{\int dz\,\rho_i(z)}{\sum_{i=1}^{2}\int dz\,\rho_i(z)}, \tag{22}$$

and represents the size selectivity of a confined binary fluid mixture. For the binary fluid mixture, the adsorption of particles with a size σ_i is preferred when the pore average mole fraction ϕ_i is greater than $\frac{1}{2}$. For a large particle size ratio the pore average mole fraction for a colloid-colloid mixture is larger than that for a polymer-polymer mixture. However, the pore average mole fraction for a colloid-colloid mixture is almost the same as that for a colloid-polymer mixture. On the other hand, for a small particle size ratio the pore average mole fraction for a colloid-polymer mixture is smaller than that for a polymer-polymer mixture. The pore average mole fraction for a polymer-polymer mixture is almost the same as that for a colloid-colloid mixture. The calculated results also

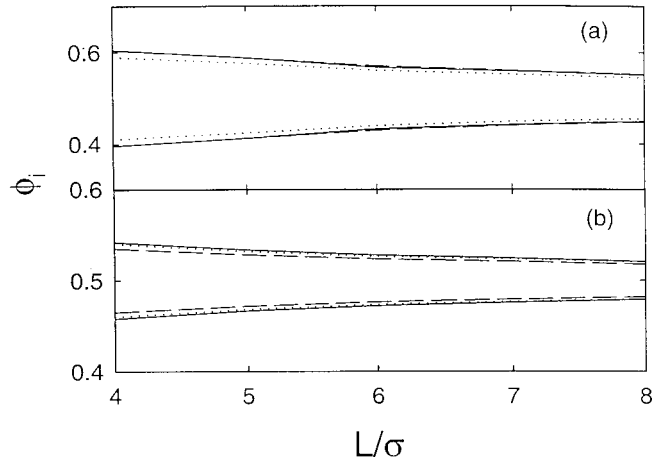

FIG. 3. (a) Pore average mole fraction ϕ_i for the binary fluid mixture, where $\eta=0.394$ and $x=0.5$; dotted lines represent a polymer-polymer mixture ($q=12$ and $\sigma_p/\sigma_p=0.5$), dashed lines a colloid-polymer mixture ($q=12$ and $\sigma_c/\sigma_p=0.5$), and solid lines a colloid-colloid mixture ($\sigma_c/\sigma_c=0.5$). (b) Same as in (a); dotted lines represent a polymer-polymer mixture ($q=12$ and $\sigma_p/\sigma_p=2.0$), dashed lines a colloid-polymer mixture ($q=12$ and $\sigma_c/\sigma_p=2.0$), and solid lines a colloid-colloid mixture ($\sigma_c/\sigma_c=2$).

show that for a small particle size ratio the pore average mole fraction is relatively smaller than that for a large particle size ratio. This means that the particle size selectivity for a binary fluid mixture increases with increasing particle size ratio in the mixture.

The calculated pore average mole fractions for three different binary mixtures are shown in Fig. 4(a) as a function of the star polymer diameter σ_p, where the diameter of a colloidal hard sphere is taken as the unit diameter $\sigma_c=\sigma$. As can be seen from Figs. 3 and 4(a), the pore average mole

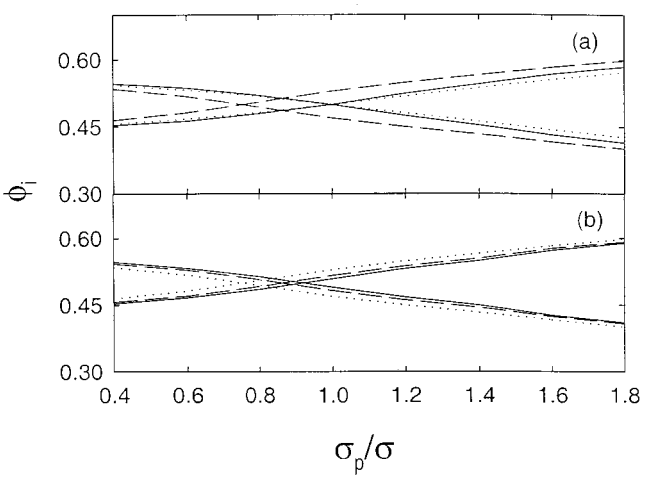

FIG. 4. (a) Pore average mole fraction ϕ_i for the binary fluid mixture, where $L=4.0\sigma$, $q=5$, $x=0.5$, $\sigma_c=\sigma$, and $\eta=0.4$; the dotted lines represent a polymer-polymer mixture, dashed lines a colloid-polymer mixture, and solid lines a colloid-colloid mixture. (b) Pore average mole fraction for a colloid-polymer mixture with the different softness, where $L=4.0\sigma$, $x=0.5$, $\sigma_c=\sigma$, and $\eta=0.4$; dotted ($q=5$), dashed ($q=15$), and solid ($q=30$) lines.

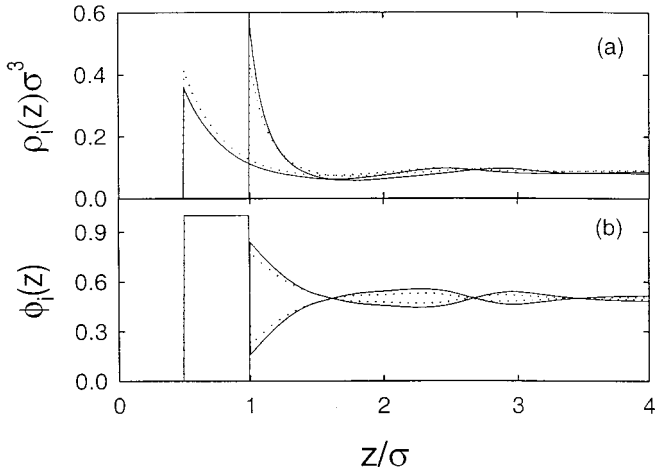

FIG. 5. (a) Equilibrium particle density distribution for the colloid-polymer mixture, where $L=8.0\sigma$, $\eta=0.394$, $x=0.5$, and $q=12$; dotted ($\sigma_p/\sigma_c=2.0$) and solid ($\sigma_p/\sigma_c=0.5$) lines. (b) Local relative concentration $\phi_i(z)$.

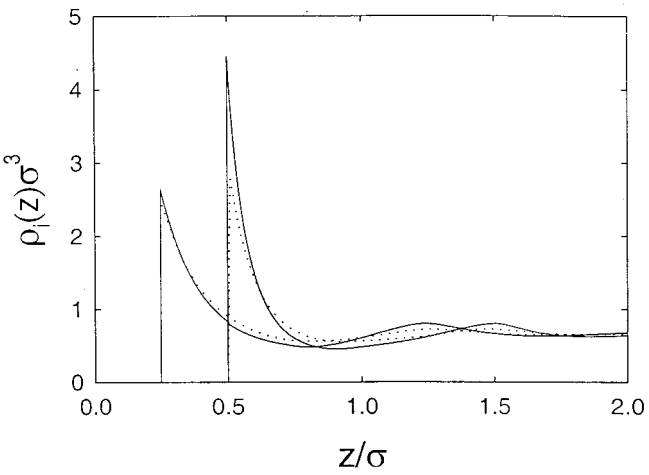

FIG. 6. Same as in Fig. 5(a); dotted ($\sigma_p/\sigma_c=2.0$) and solid ($\sigma_p/\sigma_c=0.5$) lines.

fraction shows very different size selectivities depending on the diameter of a star polymer. For colloid-colloid and polymer-polymer mixtures, the pore average mole fraction decreases with the increasing diameter of a star polymer, up to $\sigma_p=1$, and again increases with increasing σ_p when σ_p is greater than the unit of a diameter. At a large particle ratio, the adsorption for a colloid-colloid mixture is larger than that for a polymer-polymer mixture. However, one interesting thing is that for the small particle size ratio the pore average mole fraction for a colloid-polymer mixture is smaller than that for a colloid-colloid mixture, but it increases with increasing particle size ratio and exceeds those of other binary fluid mixtures. For a colloid-polymer mixture, the same pore average mole fraction $\phi_p=\phi_c$ for a colloidal hard-sphere and a star polymer has been found near $\sigma_p\sim 0.75\sigma$, due to the softness of a star polymer. The above result suggests that there seems to exist no direct relationship between the intermolecular potential and the pore average mole fraction of the binary fluid mixture. In Fig. 4(b), the pore average mole fraction for a colloid-polymer mixture with three different softnesses is displayed. As for a small particle size ratio, a colloid-polymer mixture with a high-q value shows a large pore average mole fraction, whereas for a large particle size ratio a colloid-polymer mixture with a low-q value shows a large pore average mole fraction. This means that the size selectivity of a confined colloid-polymer mixture depends not only on the particle size ratio, but also on the softness of a star polymer. In adsorption, the particle size dependence can be explained by the results of a competition between the Helmholz free energy and the chemical potential [20]. The excess free energy increases when the q value of a star polymer is increased. Then the excess free energy is more important than the chemical potential. The larger the particle size, the higher the free energy. Thus the pore average mole fraction for a colloid-polymer mixture increases with an increasing q value of a star polymer.

In Figs. 5 and 6, we show equilibrium particle density distributions for colloid-polymer mixtures with different size ratios σ_p/σ_c. The calculated result shows that the equilibrium particle density distribution depends on the softness of a star polymer in a colloid-polymer mixture. The strong repulsive interaction causes a higher density development and a strong local relative concentration near a hard wall. For a large polymer, the effect of softness is larger than that for a small polymer, and increases with an increasing particle size ratio. The distance between two particle density distributions depends on the diameter of a large particle, but not on a colloidal hard sphere and a star polymer. The calculated pore average mole fraction for colloid-polymer mixtures with different particle size ratios is shown in Fig. 7 as a function of the slit pore width L/σ. The calculated results again show that the softness of a star polymer affects the size selectivity of a colloid-polymer mixture. With an increasing diameter of a polymer, the pore average mole fraction increases. In this case, the pore average mole fraction values for small or large particles result almost linearly with an increase in the pore size.

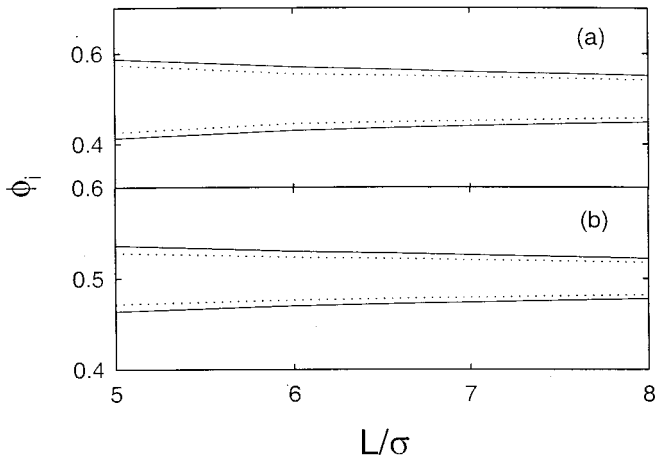

FIG. 7. (a) Pore average mole fraction for the colloid-polymer mixture, where $\eta=0.394$, $x=0.5$, and $q=12$; dotted ($\sigma_p/\sigma_c=0.5$) and solid ($\sigma_p/\sigma_c=2.0$) lines. (b) same as in (a); dotted ($\sigma_p/\sigma_c=0.5$) and solid ($\sigma_p/\sigma_c=2.0$) lines.

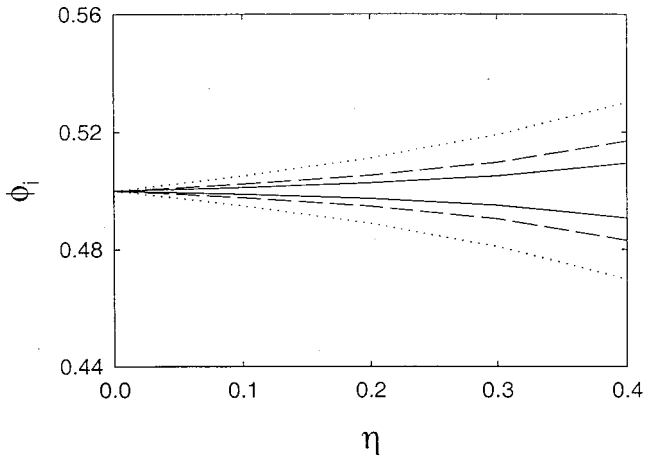

FIG. 8. Pore average mole fraction ϕ_i for a colloid-polymer mixture, where $L=4.0\sigma$, $x=0.5$, $\sigma_c=\sigma_p$, and $\eta=0.4$; dotted ($q=5$), dashed ($q=15$), and solid ($q=30$) lines.

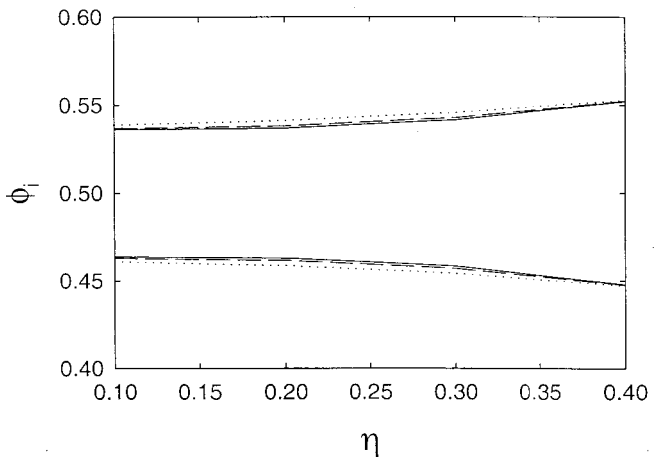

FIG. 9. Pore average mole fraction ϕ_i for a colloid-polymer mixture, where, $L=8.0\sigma$, $x=0.5$, $2\sigma_c=\sigma_p$, and $\eta=0.4$; dotted ($q=5$), dashed ($q=15$), and solid ($q=30$) lines.

The calculated pore average mole fraction for a colloid-polymer mixture with $\sigma_p/\sigma_c=1$ is presented in Fig. 8 as a function of the packing fraction η. In this case, the pole average mole fraction for a star polymer is larger than that for a colloidal hard-sphere. At a low bulk packing fraction, the pole average mole fraction approaches the bulk mole fraction $x=\frac{1}{2}$, and the softness of a star polymer does not affect the pore average mole fraction. With an increasing bulk packing fraction, the pore average mole fraction for a colloid-polymer mixture with a low-q value rapidly increases compared with colloid-polymer mixtures with a high-q value. This result explains that a large size selectivity occurs at the low-q value and at a high bulk packing fraction. This kind of result can be seen in the adsorption of a polydisperse soft-sphere fluid confined in a structureless hard pore, where it has the continuous distribution of the particle diameters [16]. The calculated pore average mole fraction for a colloid-polymer mixture with $\sigma_p/\sigma_c=2$ is presented in Fig. 9. As can be seen from this figure, the pore average mole fraction for a large particle decreases with an increasing bulk packing fraction; for a binary hard-sphere mixture confined in a hard spherical pore, the pore average mole fraction for a large particle increases with an increasing bulk packing fraction [16].

IV. CONCLUSIONS

We have employed the fundamental-measure theory for an additive binary fluid mixture to investigate the selective adsorption of binary fluid mixtures confined in a structureless hard slit pore. The adsorption for a confined colloid-polymer mixture is very different from that for colloid-colloid and polymer-polymer mixtures. For a fixed slit pore the equilibrium particle density distribution and local relative concentration depend on the intermolecular interaction between two particles and the softness of a star polymer. The size selectivity of a confined colloid-polymer mixture depends not only on the particle size ratio but also on the softness of a star polymer. The calculated result suggests that there seem to exist no general relationship between the pore average mole fraction for a binary fluid mixture and the intermolecular potential of the mixture. Here one interesting fact is that for the slit pore system the pore average mole fraction for a large particle decreases with an increasing bulk packing fraction, whereas for a closed system such as a spherical cage the pore average mole fraction for a large particle increases with an increasing bulk packing fraction. Actually, the adsorption behavior of an open system is very different from that of a closed system such as a spherical pore, where the number of particles N is fixed [16]. Another interesting point is the effect of wall deformations on the additive colloid-polymer mixture confined in a slit of deformable walls [23], and the phase separation in a star polymer-colloid mixture [24]. We will investigate these problems in the near future.

ACKNOWLEDGMENTS

This work was supported by Korea Research Foundation Grant (KRF-2000-015-DP0099), 2000 and the National Science Foundation through Grant No. CTS-9871919.

[1] Z. Tan, U. Marini Bettolo Marconi, F. van Swol, and K. E. Gubbins, J. Chem. Phys. **90**, 3704 (1989).
[2] R. Leidl and H. Wagner, J. Chem. Phys. **98**, 4142 (1993).
[3] Soon-Chul Kim, Chang Hee Lee, and Back Suck Seong, Phys. Rev. E **60**, 3413 (1999).
[4] S. Zhou, J. Chem. Phys. **113**, 8719 (2000).
[5] L. D. Gelb, K. E. Gubbins, R. Radhakrishnan, and M. Sliwinska-Bartkowiak, Rep. Prog. Phys. **62**, 1573 (1999).
[6] Y. Rosenfeld, Phys. Rev. A **42**, 5978 (1990); Y. Rosenfeld, M. Schmidt, H. Löwen, and P. Tarazona, Phys. Rev. E **55**, 4245 (1997).
[7] P. Tarazona and Y. Rosenfeld, Phys. Rev. E **55**, R4873 (1997);

B. Groh, *ibid.* **61**, 5218 (2000).
[8] M. Schmidt, Phys. Rev. E **60**, R6291 (1999); **62**, 4976 (2000).
[9] B. Groh and M. Schmidt, J. Chem. Phys. **114**, 5450 (2001).
[10] M. Schmidt, J. Phys: Condens. Matter **11**, 10 163 (1999).
[11] M. Schmidt, Phys. Rev. E **62**, 3799 (2000).
[12] C. N. Likos, H. Löwen, M. Watzlawek, B. Abbas, O. Jucknischke, J. Allgaier, and D. Richter, Phys. Rev. Lett. **80**, 4450 (1998).
[13] J. Dzubiella, A. Jusufi, C. N. Likos, C. von Ferber, H. Loewen, J. Stellbrink, J. Allgaier, D. Richter, A. B. Schofield, P. A. Smith, W. C. K. Poon, and P. N. Pusey, Phys. Rev. E **64**, 010401(R) (2001).
[14] M. Schmidt, H. Löwen, J. M. Brader, and R. Evans, Phys. Rev. Lett. **85**, 1934 (2000).
[15] Y. Rosenfeld, M. Schmidt, M. Watzawek, and H. Löwen, Phys. Rev. E **62**, 5006 (2000).
[16] Soon-Chul Kim, J. Chem. Phys. **114**, 9593 (2001).
[17] Soon-Chul Kim and Soong-Hyuck Suh, Mol. Phys. **99**, 81 (2001).
[18] R. Roth and S. Dietrich, Phys. Rev. E **62**, 6926 (2000).
[19] R. Evans, in *Fundamentals of Inhomogeneous Fluids*, edited by D. Henderson (Dekker, New York, 1992).
[20] H. T. Davis, *Statistical Mechanics of Phases, Interfaces, and Thin Films* (VCH, New York, 1996).
[21] M. Wertheim, L. Blum, and D. Bratko, in *Micellar Solutions and Microemulsions*, edited by S. H. Chen and R. Rajogopalan (Springer-Verlag, New York, 1990).
[22] I. Pagonabarraga, M. E. Cates, and G. J. Ackland, Phys. Rev. Lett. **84**, 911 (2000).
[23] J. Chakrabati, Phys. Rev. E **61**, R4698 (2000).
[24] J. M. Brader, M. Dijkstra, and R. Evans, Phys. Rev. E **63**, 041405 (2001).